THE JOURNAL OF BIOLOGICAL CHEMISTRY

Vol. 270, No. 19, Issue of May 12, pp. 11437–11444, 1995
Printed in U.S.A.

Flexibility of Actin Filaments Derived from Thermal Fluctuations

EFFECT OF BOUND NUCLEOTIDE, PHALLOIDIN, AND MUSCLE REGULATORY PROTEINS*

(Received for publication, November 10, 1994, and in revised form, January 26, 1995)

Hervé Isambert‡, Pascal Venier§, Anthony C. Maggs‡, Abdelatif Fattoum¶, Ridha Kassab¶, Dominique Pantaloni§, and Marie-France Carlier§

From the ‡Groupe de Physicochimie Théorique, Ecole Supérieure de Physique et Chimie Industrielles, Paris 75005, the §Laboratoire d'Enzymologie, CNRS, Gif-sur-Yvette 91198, and ¶Centre de Recherches de Biochimié Macromolèculaire, Montpellier 34033, France

Single actin filaments undergoing brownian movement in two dimensions were observed at 20 °C in fluorescence optical video microscopy. The persistence length (L_p) was derived from the analysis of either the cosine correlation function or the average transverse fluctuations of a series of recorded shapes of filaments assembled from rhodamine-actin. Phalloidin-stabilized filaments had a persistence length of 18 ± 1 μm, in agreement with recent observations. In the absence of phalloidin, rhodamine-labeled filaments could be observed under a variety of solution conditions once diluted in free unlabeled G-actin at the appropriate critical concentration. Such nonstabilized F-ADP-actin filaments had the same L_p of 9 ± 0.5 μm, whether they had been assembled from ATP-G-actin or from ADP-G-actin, and independently of the tightly bound divalent metal ion. In the presence of BeF_3^-, which mimics the γ-phosphate of ATP, F-ADP-BeF_3-actin was appreciably more rigid, with L_p = 13.5 μm. Hence, newly formed F-ADP-P_i-actin filaments are more rigid than "old" F-ADP-actin filaments, a fact which has implications in actin-based motility processes.

In the presence of skeletal tropomyosin and troponin, filaments were rigid (L_p = 20 ± 1 μm) in the off state ($-Ca^{2+}$), and flexible (L_p = 12 μm) in the on state ($+Ca^{2+}$), consistent with the steric blocking model. In agreement with x-ray diffraction data, no appreciable difference was recorded between the off and on states using smooth muscle tropomyosin and caldesmon (L_p = 20 ± 1 μm). In conclusion, this method allows accurate measurement of small (≤15%) changes in mechanical properties of actin filaments in correlation with their biological functions.

Actin plays a pivotal role in cell morphology and motility. The organization of actin filaments in a meshwork in the peripheral cytoplasm is responsible for the mechanical stability of living cells (1); actin filaments, associated to the family of myosin motors, generate contractile activity and translocation of endocytic vesicles within the cell (2); finally, actin filaments are dynamic polymers whose assembly can drive cell shape changes, chemotactic movement, and cell migration (3, 4). The flexural rigidity of actin filaments is central to the above basic functions, in which filaments have either to resist shearing or compressive forces of a few piconewtons, or to develop propulsive forces via self-assembly. The rigidity of filament networks appears regulated within a broad range by specific actin-binding proteins which either cross-link filaments in a rigid three-dimensional gel, enhance their intrinsic rigidity by bundling, or induce gel-sol transition by fragmentation (5). Other actin-binding proteins such as profilin, thymosin β_4, and capping proteins are more specifically involved in the regulation of filament assembly. Specifically, thymosin β_4 allows the formation of a pool of unpolymerized actin (6); the size of this pool is controlled by the concentration of free G-actin at steady state, which is itself regulated by capping proteins and profilin (7, 8). It is via the concerted control of assembly dynamics and of mechanical properties that the biological functions of actin filaments are fulfilled.

The mechanical properties of actin filaments are tightly correlated with the helical structure of the polymer, and it is expected that factors affecting the structure, and the thermodynamic stability, of the filament also affect its flexibility. The actin filament can be described as a two-start right-handed helix which displays appreciable variability in crossover periodicity (9), as observed on electron micrographs, and which has been modeled in terms of cumulative angular disorder (10, 11) or lateral slipping (12). The actin monomer itself is made of 4 subdomains (13) which undergo different types of motion relative to one another, as shown by a normal mode analysis (14). The intrinsic flexibilities of all monomers cumulate to generate the collective motion of the F-actin polymer; however, a mode analysis of the filament is not available yet. The mechanical properties of the actin monomer, hence of the filament, may be regulated by ligand binding. Of particular interest is the effect of bound nucleotide. Under physiological conditions, in the presence of ATP, filaments are made of F-ADP subunits. The bound ADP, which results from ATP hydrolysis associated to filament assembly, is nonexchangeable with medium ATP. The release of P_i following ATP hydrolysis on F-actin is linked to the destabilization of actin-actin bonds in the filament (15). P_i or analogs of P_i such as BeF_3^-, H_2O, or AlF_4^- reconstitute a very stable F-ADP-P or F-ATP-like filament with strong actin-actin bonds (16) and higher structural order (17, 18). Similarly, the drug phalloidin, which stabilizes F-actin, *i.e.* decreases the critical concentration for polymerization (19), decreases the angular spread in gels of oriented actin filaments (20), decreases the variability in crossover periodicity (12), and appears to strengthen actin-actin bonds both across and along the two-start helix (21). Finally, proteins binding to filaments and regulating contractility, such as tropomyosin, troponins, and

* This work was carried out in partial fulfillment of a Ph.D. thesis (P. V.) and was supported by the Association pour la Recherche contre le Cancer (ARC), Association Française contre les Myopathies (AFM), and the Ligue Nationale Française contre le Cancer. The costs of publication of this article were defrayed in part by the payment of page charges. This article must therefore be hereby marked "*advertisement*" in accordance with 18 U.S.C. Section 1734 solely to indicate this fact.

caldesmon, may affect the flexibility of thin filaments as part of their function.

It is therefore interesting to examine whether and how changes in thermodynamic stability of F-actin correlate with changes in filament order and in flexural rigidity.

Flexural rigidity of actin has been investigated thus far using a number of techniques that proved more or less reliable and accurate. It is to be noted that from the point of view of the polymerist actin is sufficiently rigid to be classifiable as a "semi-flexible" polymer. Most classical, artificial polymers can be classified as flexible; typically, the polymer turns many times in the solution to form a relatively compact disordered coil. Actin filament is much more rigid; however, to describe its dynamics we cannot consider the system as completely stiff, simple visual observation by video microscopy in real time shows that thermal fluctuations are still important for filaments that are longer than a few microns in length.

Early measurements of rigidity using electron microscopy are susceptible to artifacts due to inherent fixation/staining procedures and to the adsorption of the specimen to the grid. Rheological measurements (22) and dynamic light scattering (23, 24) have been used to attempt to deduce the rigidity of actin. The theory of the rheology of flexible polymers (polymers in which the persistence length is small compared with the length of the polymer and also small compared with the entanglement distance in the solution) has been extremely well developed (25). The theory of the rheological properties of semiflexible polymers is however much less developed; attempts to simply adapt the theory of flexible polymers to the case of actin have not yet been successful. Recently it has been shown that deviations observed (26) in the dynamic light scattering from the behavior of Rouse Zimm flexible chains are consistent with that expected for semiflexible chains (27). A detailed analysis allows one to deduce the rigidity to within 30% in a completely noninvasive manner; however, a number of delicate hydrodynamic corrections are needed to obtain reliable and consistent results (28).

Recent developments in video-assisted optical microscopy have prompted experiments in which the fluctuations in the shape of actin filaments undergoing brownian motion in solution are observed using the fluorescence of the bound tetramethyl rhodamine-phalloidin to visualize individual filaments. In early studies, the flexural rigidity was derived from measurements of end-to-end distance (29); however, this analysis is more appropriate for flexible than for semiflexible polymers. More precise values of the flexural rigidity were recently determined using either a mode analysis (30) or the cosine correlation function (31). In both cases, a persistence length of 17–18 μm was found for phalloidin-stabilized F-actin.

Because we thought that phalloidin might change the mechanical properties of actin, we have designed appropriate experiments to measure the flexural rigidity of native filaments without phalloidin and investigate how it can be regulated by bound nucleotide, associated proteins, and ionic conditions. A novel analysis method, using the average two-dimensional transverse fluctuations, was found to be a convenient alternative to the cosine correlation function to derive the persistence length of semiflexible chains. The values found for the persistence length are in agreement with recently published data for phalloidin-decorated F-actin; however, we show that in the absence of phalloidin actin filaments are 2-fold more flexible (L_p = 9–10 μm). Filaments are also 50% stiffer in the F-ADP-P state than in the F-ADP state. Finally, the flexibility is regulated by tropomyosin and troponin in a Ca^{2+}-dependent fashion.

MATERIALS AND METHODS

Chemicals

ATP, ADP, Ap_5A,[1] EGTA, dithiothreitol, troponins, subtilisin Carlsberg (type VIII, Catalog No. P5380), and phalloidin were from Sigma. Tetramethylrhodamine-labeled phalloidin and 5-(and 6)-carboxytetramethylrhodamine succinimidyl ester (NHSR) were from Molecular Probes. Hexokinase, catalase, and glucose oxidase were from Boehringer, beryllium sulfate and aluminum nitrate (Gold label) were from Aldrich. All other chemicals were Merck analytical grade.

Proteins

Actin was purified from rabbit muscle acetone powder (32) and isolated as CaATP-G-actin by Sephadex G-200 chromatography in G buffer (5 mM Tris Cl^-, pH 7.5, 0.2 mM dithiothreitol, 0.2 mM ATP, 0.1 mM $CaCl_2$, 0.01% NaN_3) (33).

G-actin was cleaved by subtilisin between Met^{47} and Gly^{48} essentially as described (34). Briefly, G-actin in G buffer was incubated with 0.05–0.1 unit/ml subtilisin for 20 min at 20 °C. These conditions ensured completion of the subtilisin cleavage, yielding a single homogeneous 35-kDa product and no lower molecular weight polypeptides in gel electrophoresis.

Actin was fluorescently labeled in the F-actin state using NHSR. The procedure previously described (35) yielded a labeled material containing on average 3.5–4.5 lysines modified per actin molecule, which heavily interfered with its polymerization properties. A lower labeling ratio of 0.8–1.2 on average was obtained by incubating F-actin (2.5 ml, 40–60 μm) in 50 mM PIPES, pH 6.8, 50 mM KCl, 0.1 mM $CaCl_2$, 0.2 mM ATP with 0.3 mM NHSR (20-fold less than in Ref. 35) at 20 °C. The labeling reaction was monitored spectrophotometrically in a 0.2-cm path cuvette using the 16% decrease in absorbance at 567 nm that occurs upon reaction of lysines with NHSR. Using a $\Delta\epsilon_{567} = -4000\ M^{-1}\ cm^{-1}$ derived from the difference spectra of NHSR after *versus* before reaction with excess lysine, the reaction was stopped by addition of 50 mM lysine when the decrease in absorbance at 567 nm indicated that 2 lysines per actin had reacted, *i.e.* routinely at time 40–50 min. The time course of the NHSR reaction showed no evidence for rapid specific reaction of 1 lysine; rather, the slow monotonous absorbance decrease was consistent with simultaneous titration of several residues. The labeled F-actin was pelleted by centrifugation at 400,000 × *g* for 40 min at 20 °C in a TL100 Beckman ultracentrifuge, resuspended in 2.5 ml of G buffer, and chromatographed over Sephadex G-25 PD-10 to eliminate free dye. The labeled actin contained at this point 0.8–1.2 mol of rhodamine incorporated on average per mol of actin. This ratio did not appreciably change (less than 5%) after one cycle of polymerization followed by resuspension in G buffer. After one night dialysis against G-buffer and centrifugation at 400,000 × *g*, at 4 °C for 40 min, the supernatant (rhodamine-G-actin) was drop-frozen in liquid nitrogen in fractions of 20 μl and stored at −80 °C. Subtilisin-actin was labeled with NHSR using the same procedure. It was found that labeled actin was not as efficiently cleaved by subtilisin as unlabeled actin; hence, the labeling was routinely carried out after the cleavage reaction. Hence, we cannot absolutely guarantee that the distribution of rhodamine-labeled lysines was the same on uncleaved and cleaved actins.

We preferred to label actin lysines rather than Cys^{374}, to avoid interference with the binding of F-actin binding proteins such as caldesmon.

ADP-G-actin (either unlabeled or rhodamine-labeled) was prepared according to the recently updated procedure (36) using hexokinase. ATP-G-actin (50 μM in G buffer containing 10–20 μM ATP and supplemented with 0.2 mM EGTA and 100 μM $MgCl_2$) was incubated on ice for 1 h with 30 units/ml hexokinase and 2.5 mM glucose. The solution was then supplemented with 50 μM ADP and 10 μM Ap_5A to inhibit myokinase activity (37). The ADP-G-actin was kept at 0 °C and used within the next 4 h. To polymerize actin from ADP-G-actin, the above solution of ADP-rhodamine-G-actin (50 μM, 100 μl) was brought to 20 °C and 0.1 M KCl and 1 mM $MgCl_2$ were added. Polymerization was very slow due to the poor ability of ADP-actin to nucleate (38), and the polymerization process was accelerated by fragmentation of filaments by pipetting every 5 min (~3 times) until viscosity developed in the solution. The solution of rhodamine-labeled F-actin at equilibrium in ADP was kept at 20 °C and used within the next 3–4 h.

The CaATP-G-actin in G buffer was converted into MgATP-G-actin by simultaneous additions of 0.2 mM EGTA and an amount of $MgCl_2$

[1] The abbreviations used are: Ap_5A, P^1,P^5-di(adenosine 5′)-pentaphosphate; NHSR, 5-(and 6)-carboxytetramethylrhodamine succinimidyl ester; PIPES, 1,4-piperazinediethanesulfonic acid.

equal to 1 molar eq of G-actin plus 20 μM excess.

Divalent cation-free G-actin was prepared as described (39) by adding 2 mM EDTA to a solution of G-actin in buffer G containing 2 mM ATP. Divalent cation-free actin (which contains ATP instead of metal-ATP in the nucleotide site) was polymerized by addition of 0.1 M KCl after a 2-min incubation with EDTA.

Rabbit skeletal muscle tropomyosin was prepared as described (40) and purified by hydroxylapatite chromatography (41). Smooth muscle tropomyosin (42) and caldesmon (43) were purified from fresh turkey gizzards.

Fluorescence Light Microscopy

Sample Preparation—Actin filaments were visualized by the fluorescence of either rhodamine-phalloidin or rhodamine-actin itself. To observe a single filament of 2000–4000 actin subunits, *i.e.* 5.5–11-μm length in a 50 × 50 μm field (corresponding to a 50 × 50 × 2 $(\mu m)^3$ volume of solution), the final F-actin concentration must be 10–20 nM, which is an order of magnitude lower than the critical concentration for actin assembly in physiological ionic conditions. Phalloidin greatly stabilizes filaments, *i.e.* it causes a decrease in critical concentration to a value much lower than 10–20 mM (19). Hence, F-actin assembled at 40 μM in the presence of 1 molar eq of phalloidin for 2 h can be clearly seen without fluorescent background after 2000-fold dilution in polymerization buffer. In the absence of phalloidin, filaments are stable in the presence of monomer at the critical concentration (typically 0.1–0.15 μM for ATP-actin and 1.5–2 μM for ADP-actin, under physiological conditions). Hence, in the absence of phalloidin, filaments assembled from rhodamine-actin (Mg- or Ca-actin or divalent cation free-actin) at 40–60 μM could be observed once diluted into polymerization buffer containing unlabeled G-actin at the appropriate critical concentration. This hybrid system (labeled polymer/unlabeled monomer) was necessary to avoid the background of fluorescent monomer and sufficient to keep the fluorescent filaments stable and allow their observation. Filament turnover due to monomer-polymer exchange is known to be extremely slow so that, within the 15 min following dilution of rhodamine-F-actin into unlabeled G-actin at the critical concentration, filaments remain fluorescent virtually all along their length. In fact, the loss of label from the ends did not cause any appreciable change in observable length over several minutes, for ~10-μm-long filaments, in agreement with the well known slow turnover of actin filaments (36, 44–46). Note that the same experimental design (fluorescent filaments diluted in unlabeled G-actin at the critical concentration) would also allow us to run actomyosin motility assays with native filaments in the absence of phalloidin.

Observation and Data Acquisition—Individual filaments were observed at a final concentration of ~20 nM polymerized actin in the indicated buffer. 1 mM Dithiothreitol, 100 μg/ml catalase, 10 mM glucose, and 30 μg/ml glucose oxidase were added to all buffers prior to observation, to reduce photobleaching (47). The brownian motion was restricted to two dimensions by placing the 3-μl sample between a slide and a 22 × 22 mm coverslip, both precoated with bovine serum albumin (1 mg/ml). The F-actin solution was gently flattened between the two glass surfaces to avoid breakage of filaments by shearing. Excess solution was removed, and the edges of the coverslip were sealed to the slide with Valap. The thickness of the solution was estimated to 2 μm by measuring the difference in focus between the two internal glass surfaces. Observations were made at 20 °C on a Reichert Polyvar microscope equipped with a plan apochromat-100 oil immersion objective (1.3 numerical aperture) and a G_2 Reichert filter. A 6-watt argon laser was used as a high intensity source. An attached acousticooptic modulator of the frequency and duration of illumination (<1 ms) allowed to collect images of objects undergoing rapid movement under conditions minimizing the irradiation of the sample. The beam was guided through a multimodal optic fiber submitted to a 100-Hz mechanical vibration to average out speckle occurring while the image is formed in the camera and obtain a homogeneous light distribution. Images were detected at 50 frames/s using a silicon-intensified camera (Lhesa, LHL 4046 sensitivity: 10^{-5} lux) connected to a Hamamatsu Argus 10 image processor and recorded in SVHS format. Images of filaments up to 20 μm in length were digitized manually collecting typically 20 to 25 points for a filament of 10–15 μm. Although this manual digitization is more time-consuming than the automatic skeletonization procedure, it proved to be necessary when images are not highly contrasted. This situation occurs with filaments assembled from rhodamine-actin, because rhodamine bound to actin has a lower quantum yield than rhodamine bound to phalloidin. 10 to 15 clean images of a given filament were collected every 6 ± 1 s. A total of ~100 images were collected for a given experiment. The experiment was duplicated, leading to a second pool of ~100 images. The two pools of data were analyzed separately and checked for reproducibility, then the data were cumulated, giving a total of 200 digitized filaments analyzed globally.

Evaluation of the Persistence Length

Two different methods have been used to derive the rigidity of actin filaments from the digitized images.

The energy U_f of a semiflexible chain of length L confined to two dimensions is related to the curvature $(d\theta/ds)$ in the following manner (48).

$$U_f = \frac{K}{2}\int_0^L \left(\frac{d\theta}{ds}\right)^2 \mathrm{ds} \qquad \text{(Eq. 1)}$$

where K is the flexural rigidity, related to the persistence length L_p by the following equation

$$L_p = \frac{K}{k_B T} \qquad \text{(Eq. 2)}$$

where k_B is the Boltzmann constant and T the absolute temperature.

The correlation length is so-called because it expresses the distance over which the filament bends due to thermal fluctuations. One can show that in a system confined to two dimensions, the tangential directions along the filament are correlated to the persistence length as follows:

$$< C(s) > \; = \; < \cos\,[\theta(s) - \theta(0)] > \; = e^{-|s|/2\,L_p} \qquad \text{(Eq. 3)}$$

where $<C(s)>$ is the average correlation function of the tangential directions θ, measured at each point along the curvilinear abscissa S. The angular brackets denote an average over all configurations. Thus, the filament loses memory of its initial direction $\theta(0)$ in a distance comparable to L_p. The rigidity of actin filaments was measured by fitting the average of the correlation function of the digitized shapes to this functional form. As a cross-check, we derived a second independent value of the persistence length from the measurement of average transverse fluctuations $<[D(s)]^2>$. The rationale for using this parameter is that, in contrast to average longitudinal fluctuations used in earlier works, the transverse fluctuations are highly sensitive to changes in L_p for semiflexible filaments, which are of a length comparable to L_p. This point is illustrated on Fig. 1 where a filament undergoes a small fluctuation, in which the distance of a point on abscissa s from the tangent at the origin varies from D_1 to D_2, while the corresponding longitudinal distance r does not vary much (26). The average quadratic distance can be calculated by noting that for any configuration:

$$< D(s)^2 > \; = 2\int_0^s \int_{s''}^s < \sin\,\theta(s')\,\sin\,\theta(s'') > ds'\,ds'' \qquad \text{(Eq. 4)}$$

Since $\theta(s'')$ and $\theta(s'-s'')$ are independent variables, Equation 4 can be written

$$< D(s)^2 > \; = 2\int_0^s \int_{s''}^s < \sin^2\theta(s'') > \; < \cos\,\theta(s'-s'') > ds'\,ds'' \qquad \text{(Eq. 5)}$$

Substituting the result (Equation 3) in Equation 5, we find after some calculation that

$$< [D(s)]^2 > \; = L_p^2\left[2\,\frac{s}{L_p} + \frac{16}{3}\,e\,(-s/2\,L_p) - \frac{1}{3}\,e\,(-2s/L_p) - 5\right] \qquad \text{(Eq. 6)}$$

Note that for $s << L_p$, $<D^2> \sim (s^3/3\,L_p)$ as expected (27), and for $s >> L_p$, $<D^2> \sim 2\,L_p\,s$.

Analysis of Digitized Images of Filaments

The discretized filaments were interpolated by a third order Bezier spline (49). The density of guide points in the spline was varied between 1 and 2 points per μm, to verify that the derived value of L_p was invariant and independent of the exact fitting procedure. Each fitted curve was then analyzed to find the functions $C(s)$ and $[D(s)]^2$. Averaging over many filaments allowed us to fit the average functions $<C(s)>$ and $<[D(s)]^2>$ to the functional forms 3 and 6.

Using a density of points along the filament outside the selected optimum range introduces artifacts. If the plotting point density is too high, the resulting artificial roughness makes the filament look more

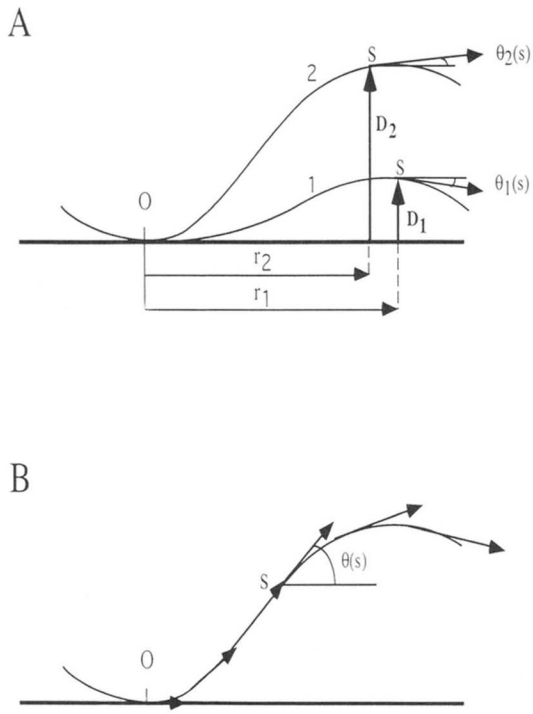

FIG. 1. **Schematic representation of thermal fluctuations of an actin filament.** *A*, transverse fluctuation. For each point of *abscissa S*, the distance *D* from the tangent at the origin is measured on a series of images. Two typical shapes, *1* and *2*, are shown. Note that *D* varies appreciably while the longitudinal distance *r* does not vary much. *B*, correlation of the tangential directions. For each point of *abscissa S*, the angle $\theta(s)$ of the tangent with the tangent at the origin is measured.

flexible at short distances while at long distances the apparent longer curvilinear distance would imply a higher stiffness. The same kind of artifact (unphysical roughness) would arise from the use of an automatic skeletonization if the plotting point density is too high (*e.g.* connected pixels) and might be responsible for the reported apparent wave vector-dependent bending stiffness of freely flickering filaments (50). On the other hand, if the plotting point density is exceedingly low, the converse effect takes place. Consideration of these artifacts enabled us to adjust the point density to obtain the best fit to theoretical curves consistent with a gaussian bending model.

The reliability of different methods for measuring the flexural rigidity can be expressed in terms of relative sensitivity to stiffness, which can be evaluated as a function of *s*:

$$w(s) = \frac{s}{<A>} \cdot \frac{d<A>}{dL_p} \qquad \text{(Eq. 7)}$$

where $<A>$ is the mean quantity which is measured. Highest values of $w(s)$ correspond to the best sensitivity. The value of w at $s = (L_p/2)$ is 0.35 for the mean transverse fluctuations $<D^2>$, and 0.5 for $\ln <\cos\theta>$, while a much lower sensitivity of 0.04 is obtained for the mean square end-to-end distance.

In this work, the same sets of data have been analyzed with the two methods (cosine correlation function and mean transverse fluctuations), and the values of the persistence length have been compared.

RESULTS

The Rigidity of Actin Filaments Is Increased 2-Fold by Phalloidin—Fig. 2 shows typical video microscopy images of filaments visualized either by tetramethylrhodamine-phalloidin decoration (*a* to *d*) or by the fluorescence of rhodamine-actin in the absence of unlabeled phalloidin (*e* to *h*). The analysis of the data using either the correlation function or the mean transverse fluctuations is shown in Fig. 3. The persistence length of actin filaments was 18 ± 1 μm once stabilized by phalloidin. The same value, within less than 5%, was obtained by the two methods and also whether unlabeled F-actin was stabilized with rhodamine-phalloidin or rhodamine-F-actin stabilized

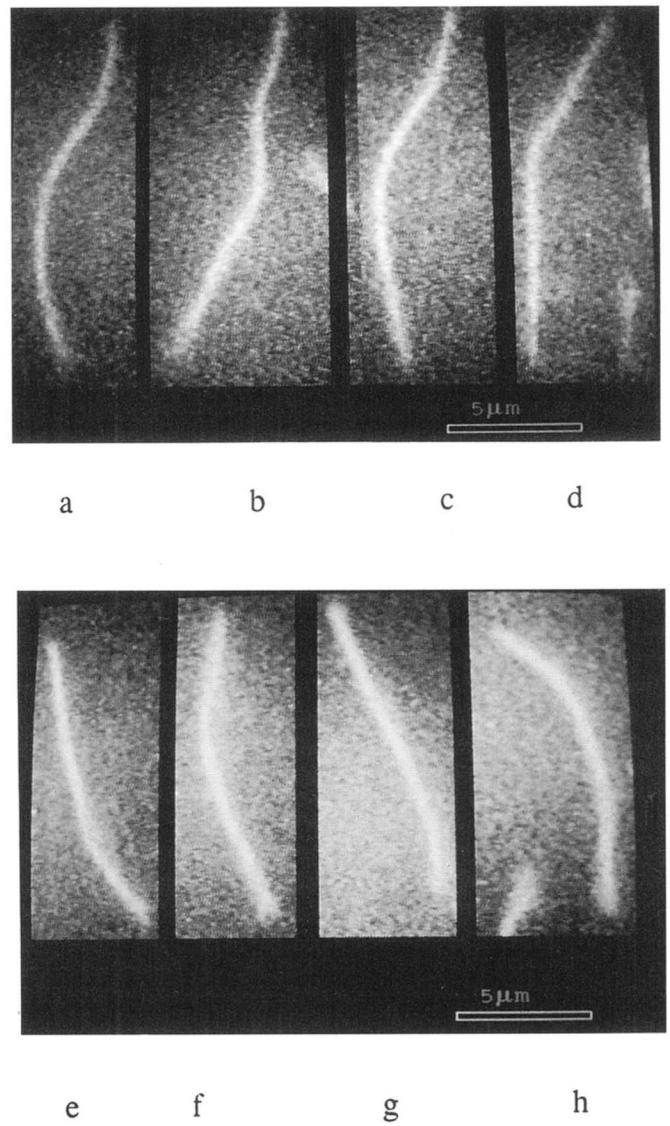

FIG. 2. **Recorded shapes of actin filaments undergoing thermal fluctuations.** *a–d*, tetramethylrhodamine-phalloidin-stabilized actin filaments observed at 6-s time intervals (*left* to *right*), *bar* = 5 μm. *c–h*, unstabilized tetramethylrhodamine-F-ADP-actin filaments observed in physiological ionic conditions at 6-s intervals in the presence of 0.2 mM ATP and 0.1 μM unlabeled G-actin.

with unlabeled phalloidin (see Table I). This number is in good agreement with the recently reported values of 17.5 μm (30) using a mode analysis and of 16.7 μm (31) using the cosine correlation function.

In the absence of phalloidin, filaments assembled from rhodamine-actin and diluted in unlabeled G-actin at the critical concentration (see "Materials and Methods") show a greater flexibility (Table I, lines 1–6). A persistence length of 9 to 10 μm was found under physiological ionic conditions. Hence, the stabilization of the filament structure by phalloidin is accompanied by a stiffening of the filament, which correlates with the better oriented fibers of F-actin obtained in the presence of phalloidin (12, 21). The identical values of the persistence length obtained for labeled and unlabeled actin, once stabilized by phalloidin, provides some warranty that labeling of actin by rhodamine has not affected the flexibility of the filament. However, some difference between labeled and unlabeled actin might have been hindered by the stabilization and rigidification due to phalloidin. Hence, the flexibility of unstabilized filaments was measured on a sample containing 80% unlabeled

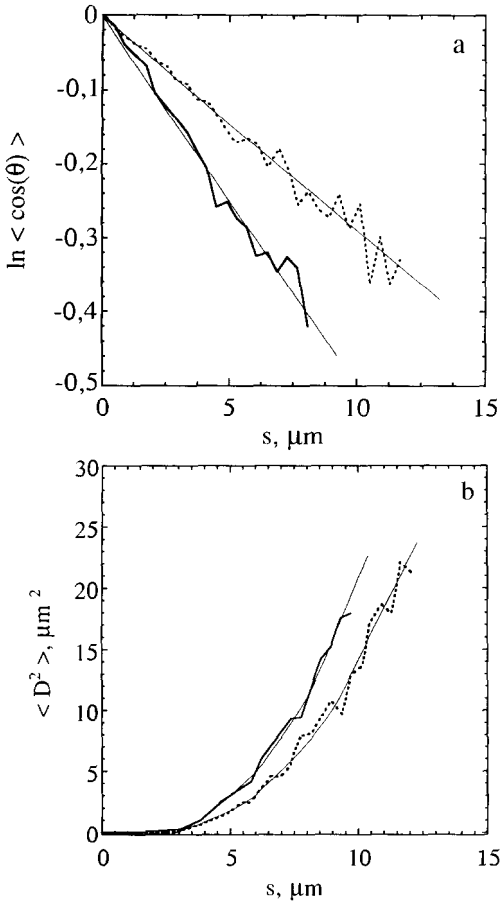

FIG. 3. **Analysis of filament flexibility.** *a*, cosine correlation function. *Dashed lines*, rhodamine-phalloidin-stabilized F-ADP-actin (conditions as under Fig. 2, *a–d*). *Solid lines*, rhodamine-F-ADP-actin in the absence of phalloidin (conditions as under Fig. 2, *e–h*). *b*, analysis of the average transverse fluctuations. *Solid* and *dashed lines* correspond to the data shown in *a*. Noisy curves are experimental data (*dashed line*, average of 263 filaments; *solid line*, average of 110 filaments). *Smooth curves* represent the best fits to Equations 3 (*a*) and 7 (*b*), respectively.

and 20% rhodamine-labeled actin (Table I, line 8), which is the lowest labeling ratio at which filaments were bright enough to be seen in the video microscope in real time. The persistence length again was 9 μm, which testifies that the incorporation of $\sim$ 1 rhodamine label on average per actin subunit does not appreciably modify the mechanical properties of actin filaments.

The technique which consists in diluting rhodamine-labeled F-actin into unlabeled (nonfluorescent) monomer at the critical concentration opens the possibility of examining the effect of different regulatory factors on actin flexibility, an effect which otherwise would be obliterated by the large stiffening effect of phalloidin.

Effect of Bound Metal Ion and Nucleotide on Filament Flexibility—Monomeric actin can have either CaATP or MgATP as bound nucleotide (16), leading to CaADP-F-actin or MgADP-F-actin as final assembly products at steady state in the presence of ATP. Rhodamine-G-actin either in the MgATP- or CaATP-bound form was assembled by addition of 0.1 M KCl into Ca-F-actin or Mg-F-actin filaments diluted prior to observation into Ca/KCl or Mg/KCl polymerization buffer (Table I, second column) containing unlabeled CaATP-G-actin or MgATP-G-actin at the respective critical concentrations of 0.6 μM or 0.1 μM (16, 51, 52). The persistence lengths were 10 μm and 9 μm for CaADP-F-actin and MgADP-F-actin, respectively, indicating that the bound metal ion does not dramatically affect the flexibility of F-actin (Table I, lines 4–6). The removal of the tightly bound metal ion by EDTA, leading to divalent cation-free actin, causes a 4–6 order of magnitude decrease in the affinity of ATP for G-actin; however, this does not greatly modify its ability to polymerize and hydrolyze ATP, leading to filaments carrying ADP and no metal ion in the nucleotide site. The persistence length of divalent cation free filament was 9 μm (Table I, line 7), *i.e.* identical with standard filaments having CaADP or MgADP as bound nucleotide. This result is in good agreement with biochemical data showing that divalent cation-free actin polymerizes with a low critical concentration (39, 53). Clearly, although the nucleotide cleft is more "open" on divalent cation-free G-actin, polymerization must drive subdomains 2 and 4 closer to each other and in interaction with a neighboring subunit, so that the final filament structure is identical, in stability and rigidity, with that of metal-ADP-F-actin.

The effect of ionic strength on filament flexibility can be assessed since F-actin can also be assembled *in vitro* in the presence of 1 mM $MgCl_2$ or $CaCl_2$. Persistence lengths of 9 μm and 8.5 μm were obtained for Mg-F-actin and Ca-F-actin under these two conditions, respectively (Table I, lines 15–16), indicating that in the range of 5–100 mM salt the flexibility of actin filaments was not affected by ionic strength.

Finally F-ADP-actin filaments can also be assembled from ADP-monomers. Filaments assembled from rhodamine-labeled MgADP-G-actin (see "Materials and Methods") and diluted in polymerization buffer containing 0.1 M KCl, 1 mM $MgCl_2$, and unlabeled MgADP-G-actin at the critical concentration of 1.5 μM (51) displayed a persistence length of 9 μm (Table I, line 9) exactly identical with the persistence length of filaments assembled from ATP subunits. This result is in agreement with thermodynamic work showing that 1) the critical concentration for actin assembly is the same when filaments have been assembled from ADP-monomers and when they have been assembled from ATP-monomers followed by ATP exhaustion from the medium (37, 38) and 2) the higher stability (lower critical concentration) of F-actin in ATP is solely due to the presence of slowly dissociating terminal F-ADP-P_i subunits at the barbed end at steady state (see Refs. 14 and 15 for review). Although an opposite view was held (54–56) by authors who reported that F-ADP-actin assembled from ADP-monomers was 5-fold more flexible than F-ADP-actin assembled from ATP-monomers, and showed a persistence length of 1 μm or less, our results fully confirm the recent reappraisals (36, 46) of those works.

We reported that, in the intermediate state F-ADP-P of ATP hydrolysis associated to actin assembly, filaments were very stable and lose subunits slowly (57, 58). This state can be mimicked using BeF_3^-, H_2O (in which beryllium has a tetrahedral coordination sphere with 3 fluoride ions and one H_2O as ligands) as a structural analog of inorganic phosphate. Electron microscopy (17, 18) showed that F-ADP-BeF_3 filaments had a highly ordered structure. The persistence length of F-ADP-BeF_3 filaments prepared as described under "Materials and Methods" was found to be 13–13.5 μm, indicating that the increased stability and order in the structure correlates with a 50% higher rigidity. The combination of phalloidin and BeF_3^- further increased the persistence length to 21 μm, showing that BeF_3^- and phalloidin have cumulative stiffening effects on the filaments. Finally, when the natural ligand P_i was used (at 30 mM, pH 7.0) to reconstitute the stable F-ADP-P_i filament, a persistence length of 11 μm was obtained, *i.e.* the rigidification of the filament was less accentuated than with BeF_3. This result may be connected to structural and biochemical data indicating that F-ADP-BeF_3 and F-ADP-P_i may represent two different conformational states of the filament consecutively along the ATP hydrolysis pathway (17, 58). The partial unrav-

TABLE I

Persistence length of actin filaments in different structural and functional states

Either unlabeled or rhodamine-labeled (Rh-)actin was assembled in filaments at 40 μM as described under "Materials and Methods" and diluted in observation buffer consisting of 5 mM Tris, pH 7.5, 0.2 mM $CaCl_2$, 0.2 mM ATP (except if nucleotide is indicated as ADP), 1 mM dithiothreitol, 10 mM glucose, 30 μg/ml glucose oxidase, 100 μg/ml catalase, and the indicated additional components (2nd column). When the stock solution of actin (40 μM) was polymerized in the Ca^{2+}-actin form, it was diluted in a calcium-containing F buffer for observation; when it was polymerized in the Mg^{2+}-actin form, it was conversely diluted in a magnesium-containing buffer. The first column describes the nature of the actin filament observed in terms of bound divalent metal ion and nucleotide, phalloidin, chemical modification, and associated proteins. The third column gives statistical information on the collection of data in terms of two numbers (N and l) = N is the number of uncorrelated configurations of filaments analyzed to derive the persistence length. However, for short curvilinear distances, each configuration of a flickering filament gives several independent data, so that the actual statistics for short distance (typically $s < 8$ to 10 μm) rely on several hundred experimental data. On the other hand, statistics for the longer curvilinear distances rely on fewer data. In the analysis, we have therefore rejected the experimental mean values averaged from less than 50 independent data, corresponding to curvilinear distances longer than a maximum length l (second number given in the third column). In the last two columns is given the persistence length of each type of filament, derived from the average transverse fluctuation ($\langle D^2 \rangle$) or from the average cosine correlation function ($\langle \cos\theta \rangle$). The following abbreviations are used: Tm, tropomyosin; Tn, troponin; CaD, caldesmon.

Sample number	Type of F-actin	Buffer additions	N/l	Persistence length derived from	
				$\langle D^2 \rangle$	$\langle \cos\theta \rangle$
			μm	μm	
1	F-MgADP-Rh-phalloidin	0.1 M KCl, 1 mM $MgCl_2$	263/15	17	17
2	F_{Rh}-MgADP-phalloidin	0.1 M KCl, 1 mM $MgCl_2$	148/13	18.5	19
3	F_{Rh}-CaADP-phalloidin	0.1 M KCl	54/12	16.5	15.5
4	F_{Rh}-MgADP	0.1 M KCl, 1 mM $MgCl_2$, 0.15 μM G-actin	110/11	9	10
5	F_{Rh}-MgADP	0.1 mM KCl, 1 mM $MgCl_2$, 0.2 mM EGTA, 0.15 μM G-actin	103/16	9	9
6	F_{Rh}-CaADP	0.1 M KCl, 0.6 μM G-actin	69/10	10	11
7	F_{Rh}-ADP (divalent cation free actin)	0.1 M KCl, 2 mM EDTA, 2 mM ATP, 0.15 μM G-actin	88/13	9	9.5
8	$F_{20\%Rh}$-MgADP	0.1 M KCl, 1 mM $MgCl_2$, 0.15 μM G-actin	62/10	8.5	9
9	F_{Rh}-MgADP assembled from G-MgADP	0.1 M KCl, 1 mM $MgCl_2$, 0.2 mM ADP, 10 μM Ap5A, 1.5 μM G-MgADP-actin	65/10	9	9
10	F_{Rh}-MgADP-BeF_3^-	0.1 M KCl, 1 mM $MgCl_2$, 100 μM $BeSO_4$, 10 mM NaF	116/13	13	13.5
11	F_{Rh}-MgADP-BeF_3^- phalloidin	0.1 M KCl, 1 mM $MgCl_2$, 100 μM $BeSO_4$, 10 mM NaF	74/13	21	20.5
12	F_{Rh}-MgADP-BeF_3 assembled from G-MgADP	0.1 M KCl, 1 mM $MgCl_2$, 100 μM $BeSO_4$, 10 mM NaF	45/10	13.5	14.5
13	F_{Rh}-Mg-ADP-P_i	0.1 M KCl, 1 mM $MgCl_2$, 30 mM P_i	96/11	10.5	11
14	F_{Rh}^{Sub}-MgADP	0.1 M KCl, 1 mM $MgCl_2$, 0.45 μM G^{Sub}-actin	137/12	18	18
15	F_{Rh}-CaADP	1 mM $CaCl_2$, 0.6 μM G-actin	36/9	8	9
16	F_{Rh}-MgADP	1 mM $MgCl_2$, 0.3 μM G-actin	36/9	8.5	9
17	F_{Rh}-MgADP Tm (skeletal muscle)	0.1 M KCl, 1 mM $MgCl_2$, 0.2 mM EGTA, 1 μM Tm	135/14	21.5	21.5
18	F_{Rh}-MgADP-Tm-Tn (skeletal muscle) off state	0.1 M KCl, 1 mM $MgCl_2$, 0.2 mM EGTA, 1 μM Tm, 1 μM Tn	130/14	19	19.5
19	F_{Rh}-MgADP-Tm-Tn-phalloidin (skeletal muscle) off state	0.1 M KCl, 1 mM $MgCl_2$, 0.2 mM EGTA, 1 μM Tm, 1 μM Tn	65/13	19	19
20	F_{Rh}-MgADP-Tm-TnCa (skeletal muscle) on state	0.1 M KCl, 1 mM $MgCl_2$, 1 μM Tm, 1 μM Tn	95/13	12	12.5
21	F_{Rh}-MgADP-Tm (smooth muscle) on state	0.1 M KCl, 1 mM $MgCl_2$, 1 μM Tm	37/10	18	18
22	F_{Rh}-MgADP-TmCAD (smooth muscle) off state	0.1 M KCl, 1 mM $MgCl_2$, 1 μM Tm, 1 μM CaD	53/12	20	20
23	F_{Rh}-MgADP-TmCAD (smooth muscle) off state	0.1 M KCl, 1 mM $MgCl_2$, 1 μM Tm, 4 μM CaD	71/15	18	18

eling of F-ADP-P_i filaments has also been noticed (12).

Proteolytic Modification of Subdomain 2 Affects Filament Rigidity—The flexible loop Pro^{38}-Ser^{52} in subdomain 2 of actin can be cleaved by several proteases, in particular subtilisin. Filaments assembled from rhodamine-labeled, subtilisin-cleaved actin were found to be highly rigid, with a persistence length of 18 μm. This twice higher rigidity than that of uncleaved F-actin filaments does not correlate with an increased stability, since subtilisin-actin actually polymerizes less well than uncleaved actin (34). Rather, this result indicates that cleavage of the flexible loop 38–52 may result in a more compact folding of this region of subdomain 2, impeding some vibrational mode of the monomer, consistent with a higher Young's modulus of the protein. The reduced motion of individual subunits sums up to generate a stiffer filament.

Tropomyosin and Troponins Rigidify Actin Filaments in a Ca^{2+}-dependent Manner: Implications in Muscle Contraction—In relaxed skeletal muscle, *i.e.* in the absence of Ca^{2+} ions, the tropomyosin-troponin complex is tightly bound to actin filaments, thus hindering the interaction with myosin heads. Contraction is triggered by Ca^{2+} binding to troponin C, which promotes a conformational change of the actin-tropomyosin-troponin that allows the binding of the myosin head to the thin filament. X-ray diffraction studies (59–61) of striated vertebrate muscles showed that reflections originating from thin filaments were clearer in the contracting than in the relaxed state, in particular, the intensity of the 2nd layer line increases upon contraction much more than the intensities of the lines at 51 Å and 59 Å. Time-resolved diffraction studies (62, 63) showed that the enhancement of the second layer line took place prior to cross-bridge attachment, hence reflecting the movement of tropomyosin on the filament; the simultaneous enhancement of the 59-Å layer line was interpreted as a possible change in filament structure linked to tropomyosin movement. Recent three-dimensional reconstructions of *Limulus* thin filaments in the "on" and "off" states (64) fully support the steric blocking model. To understand how the mechanical properties of thin filaments are involved in muscle contraction and may correlate with structural changes in actin filaments, the flexibility of rhodamine F-actin-tropomyosin-troponin thin filaments was measured in the absence (off state) and in the presence (on state) of Ca^{2+} ions.

In the absence of Ca^{2+}, thin filaments had a persistence length of 20 ± 1 μm. Tropomyosin alone (without troponin) was sufficient to stiffen the filament. The addition of phalloidin to tropomyosin-F-actin did not further increase the rigidity. When Ca^{2+} ions were present, thin filaments (tropomyosin-troponin-F-actin) became less rigid, reaching a persistence length of 12 μm. We understand, in keeping with the steric blocking model, that in the off state tropomyosin in its outer position to the filament makes a kind of rigid cage which limits the fluctuations of actin, while in the on state the inner position of tropomyosin in the groove of the double helix allows greater flexibility. The fact that thin filaments become more flexible upon

activation by Ca^{2+} may have important consequences regarding muscle function, in particular, it may provide a better positioning of the myosin heads in a functional cross-bridge attachment when the muscle fiber is Ca^{2+}-activated.

In vertebrate smooth muscle, tropomyosin and caldesmon cooperate to modulate actomyosin ATPase (65). In the absence of Ca^{2+}, caldesmon enhances the binding of tropomyosin to F-actin in the off state. Calmodulin-Ca^{2+} causes dissociation of caldesmon (on state). However, upon switching from the "off" state (with caldesmon bound) to the "on" state (in the absence of caldesmon) the change in azimuthal position of smooth muscle tropomyosin is smaller than the corresponding change for striated muscle tropomyosin (66, 67). In agreement with the above structural data, we found that 1) F-actin-smooth muscle tropomyosin filaments had the same persistence length (19 ± 1 μm) as filaments decorated with skeletal muscle tropomyosin; 2) the addition of caldesmon to smooth muscle tropomyosin-F-actin did not change the flexibility. In conclusion, the structural differences between the skeletal muscle and smooth muscle thin filaments in the on and off states correlate well with differences in the regulation of their mechanical properties.

DISCUSSION

Two main goals have been pursued in the present work. We wanted to develop methods suitable to measure the flexibility of individual actin filaments in solution and use them to quantitatively estimate how the mechanical parameters of actin filaments are regulated, in correlation with their biochemical and structural properties, by bound nucleotide, phalloidin, and associated muscle proteins. Such quantitative data are eventually useful for measuring the forces developed by actin-based myosin motors under different conditions.

The two independent analyses of the thermal fluctuations of actin filaments, the average cosine correlation function and average transverse fluctuations, yield identical values (within 5%) of the persistence length under all conditions assayed, which testifies to the validity of these methods in the analysis of semiflexible polymers and their ability to measure accurately variations of ~20% in flexibility. The data could be satisfactorily fitted to theoretical curves in a range of curvilinear distances where filaments can be considered as relatively rigid, that is up to 15 μm for stiff filaments ($L_p \sim 18$ μm) and up to 9 μm for flexible filaments ($L_p \sim 8$–9 μm). The shape fluctuations of filaments longer than 20 μm deviated significantly from the theoretical model, which may be due in part to their large dynamic two-dimensional relaxation time as compared to the sampling time of our experiments. This relaxation time may be as long as 1 h. In addition, small amplitude variations in the interaction between the filament and the glass surface, due to surface disorder, might cause trapping of very long filaments leading to metastable configurations.

The changes in flexibility of F-actin linked to ligand binding or chemical modification have interesting structural and functional implications as follows.

From a structural point of view, we note that binding of phalloidin or of the P_i analog (BeF_3^-, H_2O), which both increases the rigidity of F-actin and correlates with reported changes in the orientation of subdomain-2 (see Refs. 18, 21, and 68 for a recent review). An increase in rigidity also accompanies cleavage of loop 38–52, a modification expected to affect the structure and compactness of subdomain 2. Overall, these data indicate that subdomain-2 plays a key role as a regulatory component of the flexibility of F-actin. It would be interesting to compute how remodeling of loop 38–52 affects the normal modes of monomeric actin, and, as a consequence, of F-actin. On the other hand, in the current model of the actomyosin interface, in which the myosin head interacts with 2 adjacent actin subunits along the long pitch helix (69, 70), subdomain 2 of one of these two actins may indirectly at least interact with the myosin head; in this context, if conformational changes in subdomain 2 are induced by ATP hydrolysis on myosin, the present data suggest that changes in flexibility of F-actin might be an inherent ingredient in the mechanics of the cross-bridge. Some experimental evidence (71) supports this view.

The stiffening of F-actin linked to tropomyosin/troponin binding in the absence of Ca^{2+} (off state) and the increase in flexibility associated to Ca^{2+} binding (on state) are consistent with early quasielastic laser light scattering data (72), as well as with fluorescence polarization measurements on glycerinated fibers showing an increase in flexibility of thin filaments upon binding heavy meromyosin (73). Structural studies of muscle fibers, in particular changes in the intensities of the 51-Å and 59-Å layer lines upon binding tropomyosin were also taken as an indication that conformational changes of the small domain of actin may be involved in the mechanism of muscle contraction (74). Again, these data suggest that subdomain 2 may undergo a switch in orientation between two positions corresponding to a flexible state ($L_p \sim 9 \pm 1$ μm) and a rigid state ($L_p \sim 19 \pm 1$ μm) of the actin filament. A theoretical model involving a 25° rotation of subdomain 2 has been proposed to account for the change in flexibility of the filament (Fig. 5 in Ref. 56). Further experimental work is needed to understand the details of this switch at the atomic level and comfort the model.

From the functional point of view, the decrease in rigidity of the filament associated to P_i release following ATP hydrolysis has implications in actin-based motility processes. Incidentally, we previously found the exact same result on microtubules (75) which are 3-fold more rigid in the GDP-P_i state than in the final GDP state. It is therefore remarkable that the two major energy-dissipating polymers which organize the cell architecture could be thought of in terms of force-producing machines, since part of the mechanical energy stored in a rigid NTP or NDP-P_i polymer is restored upon P_i release and could be used to produce mechanical work.

Since P_i release from F-ADP-P_i-actin is a relatively slow process ($t_{1/2} \sim 1$ min under physiological conditions, Ref. 76), newly formed "young" F-ADP-P_i-actin filaments are stiffer than "old" F-ADP-actin filaments. As a consequence, newly assembled F-ADP-P_i filaments may provide the rigidity of the cortical actin network necessary for lamellipodial extension at the leading edge of motile cells or of the comet tail of actin filaments causing the propulsion of the bacteria *Listeria* monocytogenes and *Shigella flexneri*. F-ADP-P_i-actin filaments also offer a greater resistance to the buckling forces of myosin motors than standard F-ADP-actin filaments. It will therefore be interesting to examine how the movement of myosin heads along actin filaments is affected by nucleotide bound to actin. This issue has important *in vivo* implications since F-ADP-actin binds P_i in the millimolar range of concentrations at which P_i is known to cause muscle relaxation and loss of force (77).

Although factors acting independently of each other to increase the rigidity of actin filaments display cumulative effects (*e.g.* BeF_3 + phalloidin, or tropomyosin-troponin + phalloidin), the persistence length of actin filaments seems to have a higher limit of 21–22 μm. Hence, as previously discussed (30), the flexibility of actin filaments is in large part determined by the Young's modulus of actin, which is 1.3 to 2.9 GPa, according to our data, similar to the Young's modulus of other contractile proteins.

Acknowledgment—We thank Jean Lepault for stimulating discussions.

Note Added in Proof—In a recent study of the osmotic properties of actin (Schwienbacher, C., Magri, E., Trombetta, G., and Grazi, E. (1995) *Biochemistry* **34,** 1090–1095), changes in flexibility similar to the ones reported here have been observed upon binding of tropomyosin to F-actin and upon binding of Ca^{2+} to regulated F-actin.

REFERENCES

1. Elson, E. L. (1988) *Annu. Rev. Biophys.* **17,** 397–430
2. Cheney, R. E., and Mooseker, M. S. (1992) *Curr. Opin. Cell Biol.* **4,** 27–35
3. Bray, D., and White, J. G. (1988) *Science* **239,** 883–888
4. Condeelis, J. (1993) *Annu. Rev. Cell Biol.* **9,** 411–444
5. Janmey, P. A. (1994) *Annu. Rev. Physiol.* **56,** 169–191
6. Safer, D., and Nachmias, V. T. (1994) *BioEssays* **7,** 473–480
7. Pantaloni, D., and Carlier, M.-F. (1993) *Cell* **75,** 1007–1014
8. Carlier, M.-F., and Pantaloni, D. (1994) *Semin. Cell Biol.* **5,** 183–191
9. Hanson, J. (1973) *Proc. R. Soc. Lond. Ser. B Biol. Sci.* **183,** 39–58
10. Egelman, E. H., Francis, N., and DeRosier, D. J. (1982) *Nature* **298,** 131–135
11. Egelman, E. H., and DeRosier, D. J. (1991) *J. Mol. Biol.* **217,** 405–408
12. Bremer, A., Millonig, R. C., Sütterlin, R., Engel, A., Pollard, T. D., and Aebi, U. (1991) *J. Cell Biol.* **115,** 689–703
13. Kabsch, W., Mannherz, H. G., Suck, D., Pai, E. F., and Holmes, K. C. (1990) *Nature* **347,** 37–44
14. Tirion, M. M., and Ben-Avraham, D. (1993) *J. Mol. Biol.* **230,** 186–195
15. Korn, E. D., Carlier, M.-F., and Pantaloni, D. (1987) *Science* **238,** 638–644
16. Carlier, M.-F. (1991) *J. Biol. Chem.* **266,** 1–4
17. Lepault, J., Ranck, J. L., Erck, I., and Carlier, M.-F. (1994) *J. Struct. Biol.* **112,** 79–91
18. Orlova, A., and Egelman, E. H. (1992) *J. Mol. Biol.* **227,** 1043–1053
19. Dancker, P., Low, I., Hasselbach, W., and Wieland, T. (1975) *Biochim. Biophys. Acta* **400,** 407–414
20. Holmes, K. C., Popp, D., Gebhard, W., and Kabsch, W. (1990) *Nature* **347,** 44–49
21. Lorenz, M., Popp, D., and Holmes, K. C. (1993) *J. Mol. Biol.* **234,** 826–836
22. Janmey, P. A., Hvidt, S., Peetermans, J., Lamb, J., Ferry, J. D., and Stossel, T. P. (1988) *Biochemistry* **27,** 8218–8227
23. Fujima, S. (1972) *Adv. Biophys.* **3,** 1–43
24. Schmidt, C. F., Barman, M., Isenberg, G., and Sackman, E. (1989) *Macromolecules* **22,** 3638–3649
25. Doi, M., and Edwards, S. F. (1986) *The Theory of Polymer Dynamics*, Clarendon Press, Oxford
26. Pickenbrock, Th., and Sackman, E. (1992) *Biopolymers* **32,** 1471
27. Farge, E., and Maggs, A. C. (1993) *Macromolecules* **26,** 5041–5044
28. Janmey, P. A., Hvidt, S., Käs, J., Lerche, D., Maggs, A., Sackmann, E., Schliwa, M., and Stossel, T. P. (1994) *J. Biol. Chem.* **269,** 32503–32513
29. Takebayashi, T., Morita, Y., and Oosawa, F. (1977) *Biochim. Biophys. Acta* **492,** 357–363
30. Gittes, F., Mickey, B., Nettleton, J., and Howard, J. (1993) *J. Cell Biol.* **120,** 923–934
31. Ott, A., Magnasco, M., Simon, A., and Libchaber, A. (1994) *Phys. Rev. E.* **48,** 3, R 1642
32. Spudich, J. A., and Watt, S. (1971) *J. Biol. Chem.* **246,** 4866–4871
33. McLean-Fletcher, S., and Pollard, T. D. (1980) *Biochem. Biophys. Res. Commun.* **96,** 18–27
34. Schwyter, D., Phillips, M., and Reisler, E. (1989) *Biochemistry* **28,** 5889–5895
35. Kellogg, D. R., Mitchison, T. J., and Alberts, B. M. (1988) *Development* **103,** 675–686
36. Pollard, T. D., Goldberg, I., and Schwarz, W. H. (1992) *J. Biol. Chem.* **267,** 20339–20345
37. Pantaloni, D., Carlier, M.-F., Coué, M., Lal, A., Brenner, S., and Korn, E. D. (1984) *J. Biol. Chem.* **259,** 6274–6283
38. Carlier, M.-F., Pantaloni, D., and Korn, E. D. (1985) *J. Biol. Chem.* **260,** 6565–6571
39. Valentin-Ranc, C., and Carlier, M.-F. (1991) *J. Biol. Chem.* **266,** 7668–7675
40. Bailey, K. (1948) *Biochem. J.* **43,** 271–279
41. Eisenberg, E., and Kielley, W. W. (1974) *J. Biol. Chem.* **249,** 4742–4748
42. Bretscher, A. (1984) *J. Biol. Chem.* **259,** 12873–12880
43. Bartegi, A., Fattoum, A., and Kassab, R. (1990) *J. Biol. Chem.* **265,** 2231–2237
44. Martonosi, A., Gouvea, M. A., and Gergely, J. (1960) *J. Biol. Chem.* **235,** 1700–1711
45. Moos, C. E., Eisenberg, E., and Estes, J. E. (1967) *Biochim. Biophys. Acta* **147,** 536–545
46. Newman, J., Zaner, K. S., Schick, K. L., Gershman, L. C., Selden, L. A., Kinosian, H. J., Travis, J. L., and Estes, J. E. (1993) *Biophys. J.* **64,** 1559–1566
47. Kishino, A., and Yanagida, T. (1988) *Nature* **334,** 74–76
48. Landau, L. D., and Lifshitz, E. M. (1980) *Statistical Physics*, 3rd Ed, Part I, Pergamon Press, Oxford
49. Rogers, D. F., and Adams, J. A. in *Mathematical Elements for Computer Graphics*, 2nd Ed, Chap. 5, McGraw Hill, Inc., New York
50. Kaes, J., Strey, H., Baermann, M., and Sackman, E. (1993) *Europhys. Lett.* **21,** 865–870
51. Pollard, T. D., and Cooper, J. A. (1986) *Annu. Rev. Biochem.* **55,** 987–1035
52. Carlier, M.-F., Pantaloni, D., and Korn, E. D. (1986) *J. Biol. Chem.* **261,** 10778–10784
53. Gershman, L. C., Estes, J. E., and Selden, L. A. (1987) *Ann. N. Y. Acad. Sci.* **438,** 264–267
54. Janmey, P. A., Hvidt, S., Oster, J., Lamb, J., Stossel, T. P., and Hartwig, J. H. (1990) *Nature* **347,** 95–99
55. Burlacu, S., Janmey, P. A., and Borejdo, J. (1992) *Am. J. Physiol.* **262,** C569–C577
56. Orlova, A., and Egelman, E. H. (1993) *J. Mol. Biol.* **232,** 334–341
57. Carlier, M.-F., and Pantaloni, D. (1988) *J. Biol. Chem.* **263,** 817–825
58. Combeau, C., and Carlier, M.-F. (1989) *J. Biol. Chem.* **264,** 19017–19021
59. Huxley, H. E. (1972) *Cold Spring Harbor Symp. Quant. Biol.* **37,** 361–376
60. Haselgrove, J. C. (1972) *Cold Spring Harbor Symp. Quant. Biol.* **37,** 341–352
61. Parry, D. A. D., and Squire, J. M. (1973) *J. Mol. Biol.* **75,** 33–55
62. Wakabayashi, K., Tanaka, H., Amemiya, Y., Fujishima, A., Kobayashi, T., Toshiaki, H., Sugi, H., and Mitsui, T. (1985) *Biophys. J.* **47,** 847–850
63. Kress, M., Huxley, H. E., Farugi, A. R., and Hendrix, J. (1986) *J. Mol. Biol.* **188,** 325–342
64. Lehman, W., Craig, R., and Vibert, P. (1994) *Nature* **368,** 65–67
65. Marston, S. B., and Redwood, C. S. (1993) *J. Biol. Chem.* **268,** 12317–12320
66. Popp, D., and Holmes, K. C. (1992) *J. Mol. Biol.* **224,** 65–76
67. Vibert, P., Craig, R., and Lehman, W. (1993) *J. Cell Biol.* **123,** 313–321
68. Bremer, A., Henn, C., Goldie, K. N., Engel, A., Smith, P. R., and Aebi, U. (1994) *J. Mol. Biol.* **242,** 683–700
69. Rayment I., Holden, H. M., Whittaker, M., Yohn, C . B., Lorenz, M., Holmes, K. C., and Milligan, R. A. (1993) *Science* **261,** 58–65
70. Valentin-Ranc, C., Combeau, C., Carlier, M. F., and Pantaloni, D. (1991) *J. Biol. Chem.* **266,** 17872–17879
71. Ménétret, J.-F., Hofmann, W., Schröder, R. R., Rapp, G., and Goody, R. S. (1991) *J. Mol. Biol.* **219,** 139–144
72. Ishiwata, S., and Fujime, S. (1972) *J. Mol. Biol.* **68,** 511–522
73. Yanagida, T., and Oosawa, F. (1978) *J. Mol. Biol.* **126,** 507–524
74. Popp, D., Maeda, Y., Stewart, A. A. E., and Holmes, K. C. (1991) *Adv. Biophys.* **27,** 89–103
75. Venier, P., Maggs, A. C., Carlier, M.-F., and Pantaloni, D. (1994) *J. Biol. Chem.* **269,** 13353–13360
76. Carlier, M.-F., and Pantaloni, D. (1986) *Biochemistry* **25,** 7789–7792
77. Hibberd, M. G., and Trentham, D. R. (1986) *Annu. Rev. Biophys. Chem.* **15,** 119–161